

Compression Deformability of Γ and ζ Fe-Zn Intermetallics to Mitigate Detachment of Brittle Intermetallic Coating of Galvannealed Steels

Norihiko L. Okamoto^{1,2,*}, Daisuke Kashioka¹, Masahiro Inomoto¹, Haruyuki Inui^{1,2}, Hiroshi Takebayashi³, Shu Yamaguchi⁴

¹*Department of Materials Science and Engineering, Kyoto University, Sakyo-ku, Kyoto 606-8501, Japan*

²*Center for Elements Strategy Initiative for Structure Materials (ESISM), Kyoto University, Sakyo-ku, Kyoto 606-8501, Japan*

³*Nippon Steel & Sumitomo Metal Corporation, Ltd., 1-8 Fuso-cho, Amagasaki, Hyogo 660-0891, Japan*

⁴*Department of Materials Engineering, University of Tokyo, 7-3-1 Hongo, Bunkyo-ku, Tokyo 113-8656, Japan*

*Corresponding Author Contact Information:

Norihiko L. Okamoto
Department of Materials Science and Engineering, Kyoto University
Sakyo-ku, Kyoto 606-8501, Japan
Tel: +81-75-753-5481
Fax: +81-75-753-5461
E-mail: okamoto.norihiko.7z@kyoto-u.ac.jp

Abstract

Micropillar compression tests made for each of the five intermetallic phases of the Fe-Zn system, which constitute the coating of galvannealed steels, have revealed that the Γ phase formed in direct contact with the steel substrate and the ζ phase formed on the outermost surface are ductile, sandwiching the other three brittle phases (Γ_1 , δ_{1k} and δ_{1p}). Compression deformability of these ductile phases is considered to mitigate the coating failure through sustaining ruptured fragments of the brittle phases during the forming process.

Keywords: compression test; focused ion beam (FIB); iron alloys; multilayers; plastic deformation.

Steel is undoubtedly the most widely used structural materials because of its low cost, strength, formability and so on. When steel is used in a corrosive environment, metallic coatings and/or paints are applied for rust prevention. In automobile industries, zinc coating is usually used to prevent steels used in the automobile body from rusting caused by aqueous corrosion. The shielding mechanism is called “galvanic protection”, in which the substrate steel is cathodically protected by the sacrificial corrosion of the zinc coating because zinc is less noble (more electronegative) than iron.

The zinc-coated (galvanized) steel is sometimes subsequently heat-treated (galvannealed: GA) to alloy the zinc coating with the substrate iron through diffusion, in order to improve coating adhesion, paintability and weldability [1]. The coating layer of GA steel consists of thin layers (at most, a few micrometers for each of the layers) of intermetallic compounds of the Fe-Zn system (Γ ($\text{Fe}_3\text{Zn}_{10}$), Γ_1 ($\text{Fe}_{11}\text{Zn}_{40}$), δ_{1k} (FeZn_7), δ_{1p} (FeZn_{10}) and ζ (FeZn_{13}) [2-6] in the decreasing order of the iron content, see Figure 1a), which are formed according to the Fe-Zn binary phase diagram (see Figure S1 in the Supplementary Information (SI)). When referring to their complex crystal structures (Figure S2 in SI) [7-10] all of these Fe-Zn intermetallic phases are believed to exhibit poor deformability. This is easily expected from the very low values of the h/b ratio for these intermetallic compounds when judged from the Peierls-Nabarro stress, τ_p , which is given by [11, 12]

$$\tau_p = \frac{2\mu}{1-\nu} \exp\left(-\frac{2\pi h}{(1-\nu)b}\right), \quad (1)$$

where μ , ν , h and b stand for the shear modulus, Poisson’s ratio, interplanar distance of slip plane and magnitude of Burgers vector, respectively. A low value of the h/b ratio leads to a high Peierls-Nabarro stress for dislocation motion, generally resulting in material brittleness. The h/b ratios for all these Fe-Zn intermetallic compounds (0.059–0.180) are considerably smaller than that for iron (0.817) (see Table S1 in SI). In fact, the coating of GA steel sometimes fails by decohesion at the coating/substrate interface (flaking) or by intracoating

cracking to form fine particles (powdering) during forming process. Nevertheless, GA steels can be bent, stretched and drawn under optimized forming conditions without serious coating failure.

This has been achieved by empirically establishing the manufacturing procedures for GA steels [13]. When the heat-treatment temperature/time is insufficiently low/short, the overall iron concentration in the coating layer is low, resulting in relatively soft coatings that consist mostly of the ζ phase and unalloyed zinc. Then, the friction coefficient between the coating and stamping tools is high, making the coating layer easily flaked off from the substrate (flaking). When the heat-treatment is excessive, on the other hand, the overall iron concentration in the coating layer is high, resulting in relatively hard coatings that contain a high proportion of the Γ and Γ_1 phases. The high hardness of the coatings results in intracoating cracking to form fine particles (powdering), which eventually foul the forming dies. The optimum formability is thus generally achieved under intermediate heat-treatment conditions, avoiding severe flaking and powdering (see Figure 1b). In this case, the coating layer consists mostly of the δ_1 (δ_{1k}/δ_{1p}) phase. Because of this, the δ_1 phase has been believed to be relatively ductile, while the Γ (Γ/Γ_1) phase extremely brittle [14]. However, these empirical conclusions have never been scientifically proved yet, except that Hong et al. [15, 16] reported that none of the five intermetallic compounds exhibits plasticity in a polycrystalline form unless the temperature is raised above 200°C. In this sense, mitigated detachment of brittle intermetallic coating of GA steel during forming has been a mystery remained unsolved for a long time, in spite of the huge industrial production in the past.

It is difficult to obtain a single-phase microstructure for each of the five intermetallic compounds of the Fe-Zn system because each phase is formed via a series of peritectic/peritectoid reactions (Figure S1 in SI) [2-4]. In addition, each phase formed in the coating layer of GA steel is very thin (at most a few micrometers). These are the primary reasons for the difficulties in elucidating the mechanical properties of the respective phases.

However, recent advances in fabrication processes with precise control of material dimensions down to the nanometer level, for example, with the focused ion beam (FIB) method have made it possible to investigate mechanical properties at these small scales [17-20]. We investigate the compression deformation behaviour of FIB-fabricated micropillar specimens cut from each of the five intermetallic phases in the GA coating at room temperature, in order to elucidate the mechanical properties for the respective phases. Single-phase square columnar specimens 3.0–4.0 μm on a side with an aspect ratio of 1:3–1:4 were machined from heat-treated GA steels by using a JEOL JIB-4000 FIB at an operating voltage of 30 kV and a beam current of 100–300 pA (see Experimental Procedures in SI). Uniaxial compression tests were conducted with a flat punch indenter tip in a Shimadzu MCT-211 micro compression tester at room temperature. The compression tests were performed with a constant stress rate of 1–3 MPa s^{-1} , which corresponds to a nominal strain rate of 3×10^{-5} – $3 \times 10^{-4} \text{ s}^{-1}$ in the elastic deformation region. Figure 2 shows scanning electron microscope (SEM) images of single-phase polycrystalline micropillar specimens before (top row) and after (middle row) compression tests together with stress-strain curves obtained in compression (bottom row). While failure occurs at a stress level as high as 1,200 MPa without any appreciable plastic strain for the Γ_1 , δ_{1k} and δ_{1p} phases (Figures 2b–d), some plastic deformability is obviously observed for the Γ and ζ phases, accompanied by the appearance of deformation markings (slip lines) (Figures 2a and 2e). This is completely opposite to what has been empirically believed; the δ_1 phase is relatively ductile, while Γ phase is extremely brittle [14].

Values of plastic strain measured for several polycrystalline micropillars are plotted in Figure 3a for each of the five phases. Needless to say, plastic strain at failure is essentially zero for the Γ_1 , δ_{1k} and δ_{1p} phases. While the Γ phase exhibits deformability generally larger than 4%, the ζ phase exhibits a rather limited deformability of about 0.5%. In order to account for the limited deformability of the ζ phase, compression tests were carried out also with the

use of micropillars cut from a single crystal grown by a flux method. Unlike in polycrystalline micropillars, the ζ phase exhibits considerably large deformability exceeding 20% in single-crystalline micropillars (Figure 3c). Slip trace analysis made for deformed single-crystalline micropillars indicates that slip occurs by the operation of the $\{1\bar{1}0\}\langle 112\rangle$ slip system for a wide range of crystal orientation. If this slip system has a critical resolved shear stress considerably smaller than any other slip systems, the number of independent slip systems is only two for the ζ phase with the monoclinic unit cell (space group: $C2/m$) [10, 21, 22]. The reason for the limited deformability in polycrystalline micropillars of the ζ phase is thus due to the insufficient number of independent slip systems that are required to undergo an arbitrary imposed plastic deformation (von Mises criterion) [23, 24]. On the other hand, slip trace analysis similarly made for deformed single-crystalline micropillars of the Γ phase with the cubic unit cell (space group: $I\bar{4}3m$) [7, 9, 22] indicates that slip occurs by the operation of the $\{1\bar{1}0\}\langle 111\rangle$ slip system for a wide range of crystal orientation (Figure 3b). Then, the von Mises criterion is satisfied by the Γ phase, and a relatively large plastic strain is expected to be achieved even in a polycrystalline form, which is in contrast to the case of the ζ phase. Indeed, plastic strain at failure is as high as more than 15% for single-crystalline micropillars and is also as high as 4% for polycrystalline micropillars.

With the knowledge of the deformability for the respective phases, crack initiation and propagation in the coating of GA steel upon forming can be schematically drawn as in Figure 4. The brittle three phases, Γ_1 , δ_{1k} and δ_{1p} , are sandwiched by the relatively ductile (deformable) Γ and ζ phases. The most ductile phase, Γ , is formed in direct contact with the steel substrate, transferring the deformation occurred in the steel substrate into the coating without forming severe cracking along the coating/substrate interface. During the deformation transfer, cracks may nucleate and propagate in the three brittle phases, Γ_1 , δ_{1k} and δ_{1p} somehow severely, but ruptured fragments of these three phases may be held in the coating

because of the deformability of the ζ phase (formed on the outermost surface), avoiding the occurrence of severe powdering. As far as the layer thickness of the ζ phase in the coating is small enough, the flaking resistance may not increase significantly. We believe that this is the reason why the optimum formability of GA steels is generally achieved under intermediate heat-treatment conditions, by which the coating layer consists mostly of the δ_1 (δ_{1k}/δ_{1p}) phase.

Tensile tests are currently under way for micropillars for each of the five intermetallic phases of the Fe-Zn system in our research group. Improvements in formability of GA steels have long been waited, by which it becomes possible to produce severely shaped manufactures, for example, wavy roofing panels and highly stretched automotive fenders [25]. With the knowledge of yield strength, fracture strength, deformability and so on obtained in both tension and compression, we plan to provide an optimum phase constitution and microstructure of GA steels with the aid of the finite element method.

In summary, we reveal that the Γ phase is the most deformable followed by the ζ phase, while the Γ_1 , δ_{1k} and δ_{1p} phases are all considerably brittle from compression tests made for micrometer-sized single-phase specimens fabricated from each of the five intermetallic phases by the FIB method. These results are completely different from what has been believed empirically. A long-standing mystery about mitigated detachment of brittle coating of GA steels has now been solved; the ductile Γ phase formed in direct contact with the steel substrate and the ζ phases formed on the outermost surface sandwich the brittle Γ_1 , δ_{1k} and δ_{1p} phases, holding ruptured fragments of these three brittle phases in the coating by their plastic deformation. Our findings will provide new insights into novel design approaches to optimum microstructures of the coating layer for better coating adhesion and formability.

This work was supported by JSPS KAKENHI (No. 24246113) and the Elements Strategy Initiative for Structural Materials (ESISM) from the Ministry of Education, Culture, Sports, Science and Technology (MEXT) of Japan, and in part by Advanced Low Carbon

Technology Research and Development Program (ALCA) from the Japan Science and Technology Agency (JST). This work was also supported by Research Promotion Grant from ISIJ, and Grants for Technical Research from JFE 21st Century Foundation.

Supplementary information associated with this article can be found in the online version.

References

- [1] A.R. Marder, *Prog. Mater Sci.*, 45 (2000) 191-271.
- [2] O. Kubaschewski, *Iron - Binary Phase Diagrams*, Springer-Verlage, 1982.
- [3] X.P. Su, N.Y. Tang, J.M. Toguri, *J. Alloys Compd.*, 325 (2001) 129-136.
- [4] J. Nakano, D.V. Malakhov, G.R. Purdy, *Calphad*, 29 (2005) 276-288.
- [5] R. Kainuma, K. Ishida, *Tetsu to Hagane*, 91 (2005) 349-355.
- [6] P. Villars, *Pearson's Handbook: Crystallographic Data for Intermetallic Phases*, ASM International, Amsterdam, 1997.
- [7] J.K. Brandon, R.Y. Brizard, P.C. Chieh, R.K. Mcmillan, W.B. Pearson, *Acta Crystallogr. B*, 30 (1974) 1412-1417.
- [8] A.S. Koster, J.C. Schoone, *Acta Crystallogr. B*, 37 (1981) 1905-1907.
- [9] C.H.E. Belin, R.C.H. Belin, *J. Solid State Chem.*, 151 (2000) 85-95.
- [10] P.J. Gellings, E. Willemdebree, G. Gierman, *Z. Metallkd.*, 70 (1979) 315-317.
- [11] R. Peierls, *Proc. Phys. Soc.*, 52 (1940) 34-37.
- [12] F.R.N. Nabarro, *Proc. Phys. Soc.*, 59 (1947) 256-272.
- [13] C. Kato, H. Koumura, Y. Uesugi, K. Mochizuki, in: A.R. Marder (Ed.) *TMS Annual Meeting, The Physical Metallurgy of Zinc Coated Steel*, TMS, San Francisco, CA, 1994, pp. 241-249.
- [14] J. Mackowiak, N.R. Short, *Inter. Metals Rev.*, 24 (1979) 1.
- [15] M.H. Hong, H. Saka, *Philos. Mag. A*, 74 (1996) 509-524.
- [16] M.H. Hong, H. Saka, *Acta Mater.*, 45 (1997) 4225-4230.
- [17] D.M. Dimiduk, M.D. Uchic, T.A. Parthasarathy, *Acta Mater.*, 53 (2005) 4065-4077.
- [18] M.D. Uchic, D.M. Dimiduk, J.N. Florando, W.D. Nix, *Science*, 305 (2004) 986-989.
- [19] M.D. Uchic, P.A. Shade, D.M. Dimiduk, *Annu. Rev. Mater. Res.*, 39 (2009) 361-386.
- [20] J.R. Greer, J.T.M. De Hosson, *Prog. Mater Sci.*, 56 (2011) 654-724.
- [21] R. Belin, M. Tillard, L. Monconduit, *Acta Crystallogr. C*, 56 (2000) 267-268.

- [22] T. Hahn, *International Tables for Crystallography, Vol. A: Space-group symmetry*, 5th ed., Springer, Dordrecht, The Netherlands, 2005.
- [23] R. von Mises, *Z. Angew. Math. Mech.*, 8 (1928) 161-185.
- [24] G.W. Groves, A. Kelly, *Philos. Mag.*, 8 (1963) 877-887.
- [25] *International Zinc Association, GalvInfo Notes*,
http://www.galvinfo.com/galv_info_notes.htm 2010.

Figure Captions

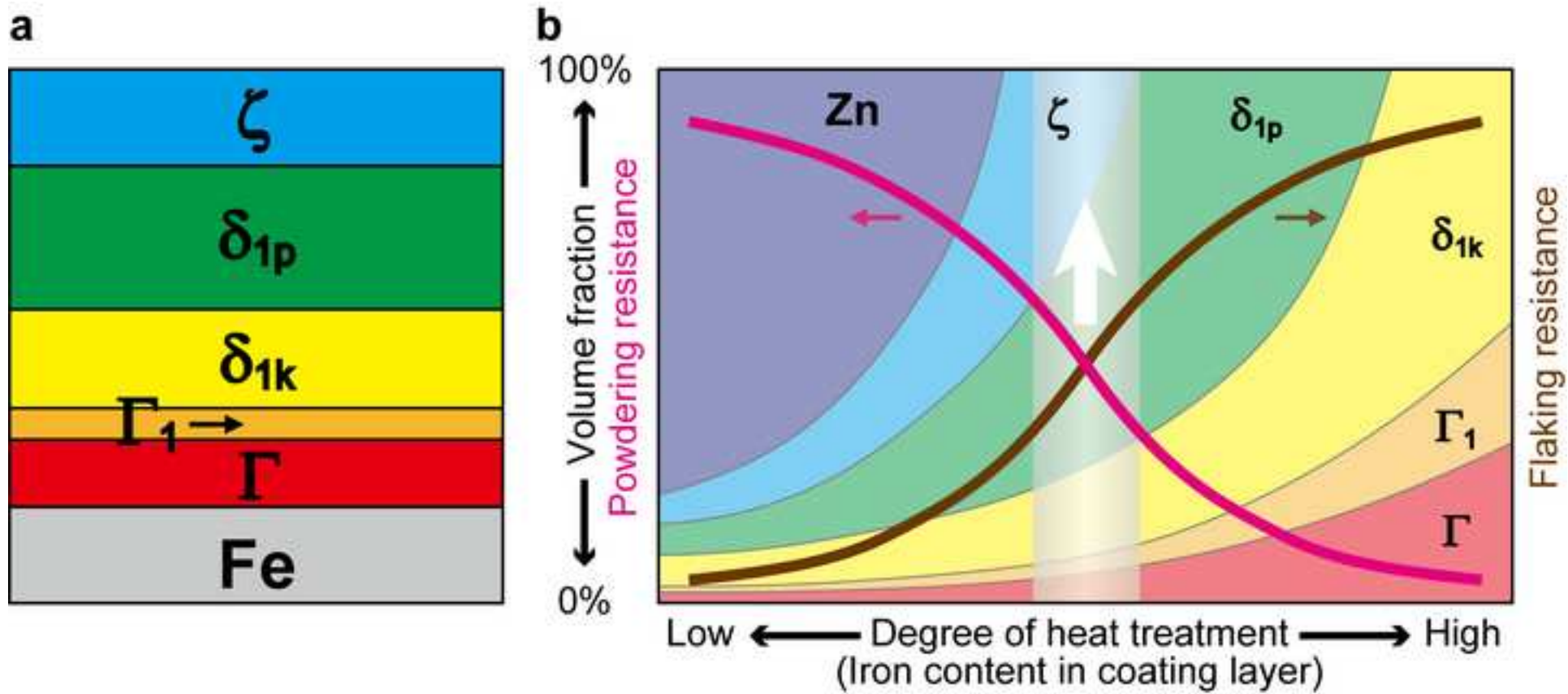
Figure 1. (Color on the Web and in print) (a) Cross-sectional view of GA steel sheet before forming. A series of Fe-Zn intermetallic compounds, Γ ($\text{Fe}_3\text{Zn}_{10}$), Γ_1 ($\text{Fe}_{11}\text{Zn}_{40}$), δ_{1k} (FeZn_7), δ_{1p} (FeZn_{10}) and ζ (FeZn_{13}), form thin layers in the coat according to the corresponding phase diagram [2-5]. (b) Phase constitution and coating properties of GA steel sheet as a function of degree of heat-treatment. The volume fraction of each intermetallic phase in the coating layer is schematically shown as a function of degree of heat-treatment (annealing temperature and time, in other words, the iron content in the coating layer). As the degree of heat-treatment augments, the flaking resistance increases due to increased coating adhesion while the powdering resistance decreases due to the embrittlement of the coating constituents. The optimum formability is generally achieved in an intermediate heat-treatment condition (in the vertical grey band) so as to strike a good balance between the flaking and powdering resistances.

Figure 2. (Color on the Web and in print) Appearance of micropillar specimens and stress-strain curves. (a) Γ , (b) Γ_1 , (c) δ_{1k} (d) δ_{1p} , and (e) ζ phases. SEM secondary-electron images of polycrystalline single-phase micropillar specimens before (top row) and after (middle row) compression tests. (bottom row) Stress-strain curves of polycrystalline single-phase micropillar specimens. The symbol \times indicates the stress at which failure occurred.

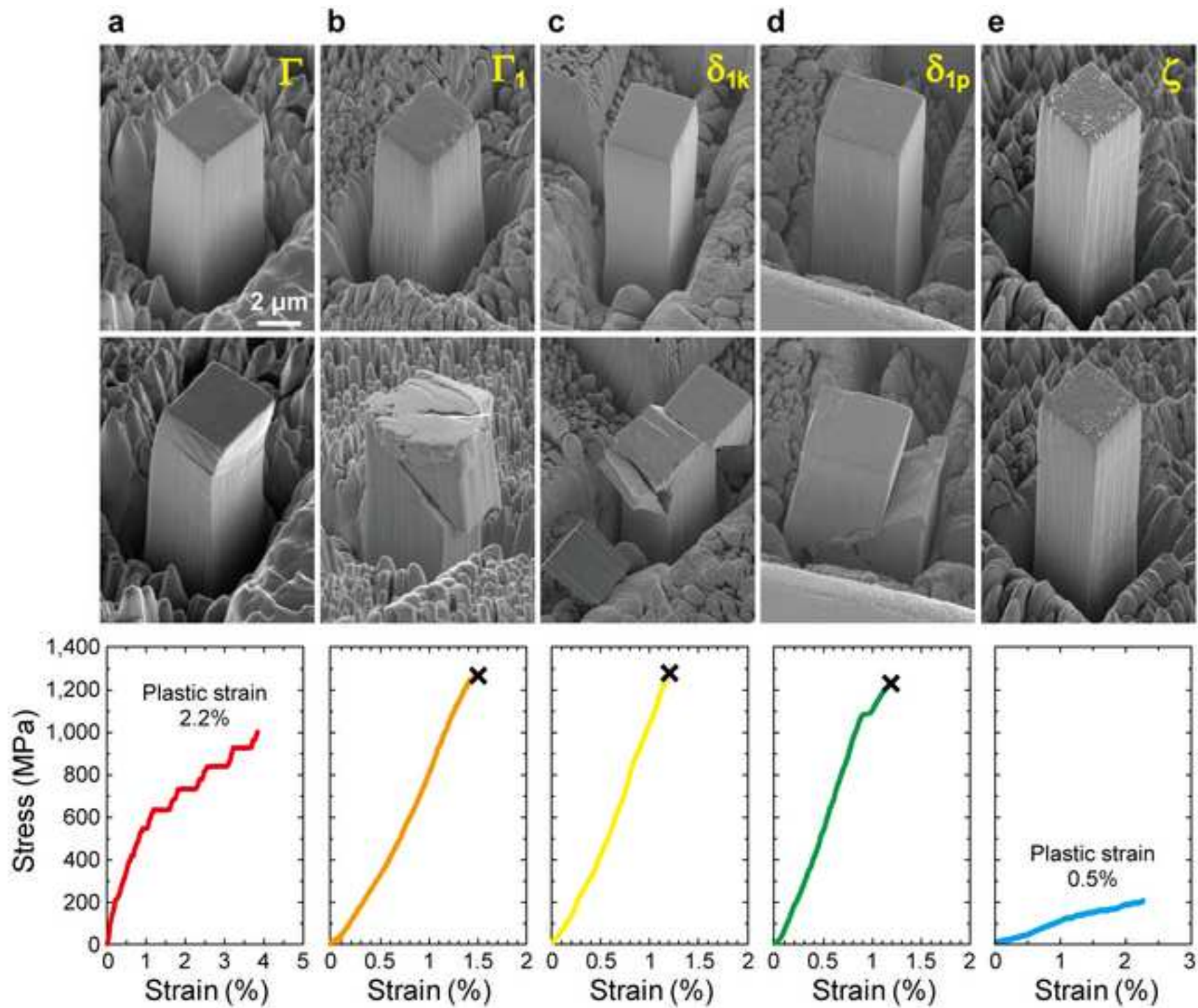
Figure 3. (Color on the Web and in print) Compression deformability of micropillar specimens for Fe-Zn compounds. (a) Values of plastic strain measured for polycrystalline (all the five phases) and single-crystalline (Γ and ζ phases) micropillars. Solid circles represent plastic strain at which failure occurred, while open ones represent plastic strain at which the compression test was interrupted before failure occurs. SEM secondary-electron images of single-crystalline micropillar specimens of the (b) Γ and (c) ζ phases after compression.

Figure 4. (Color on the Web and in print) Cross-sectional view of GA steel sheet after forming. Cracks are introduced in the brittle Γ_1 , δ_{1k} and δ_{1p} phases during forming. The ductile

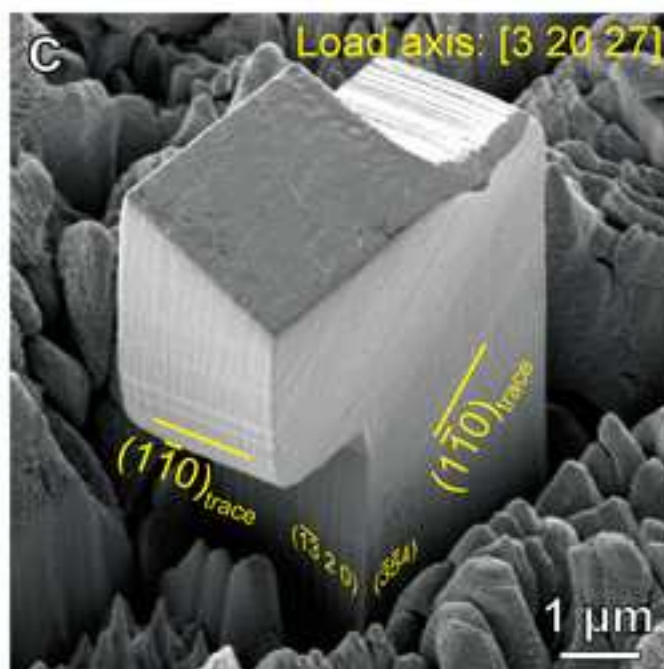
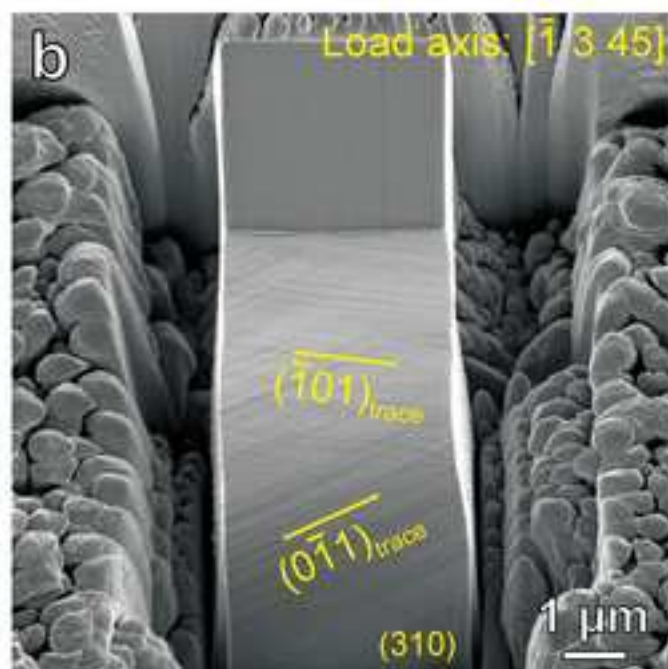
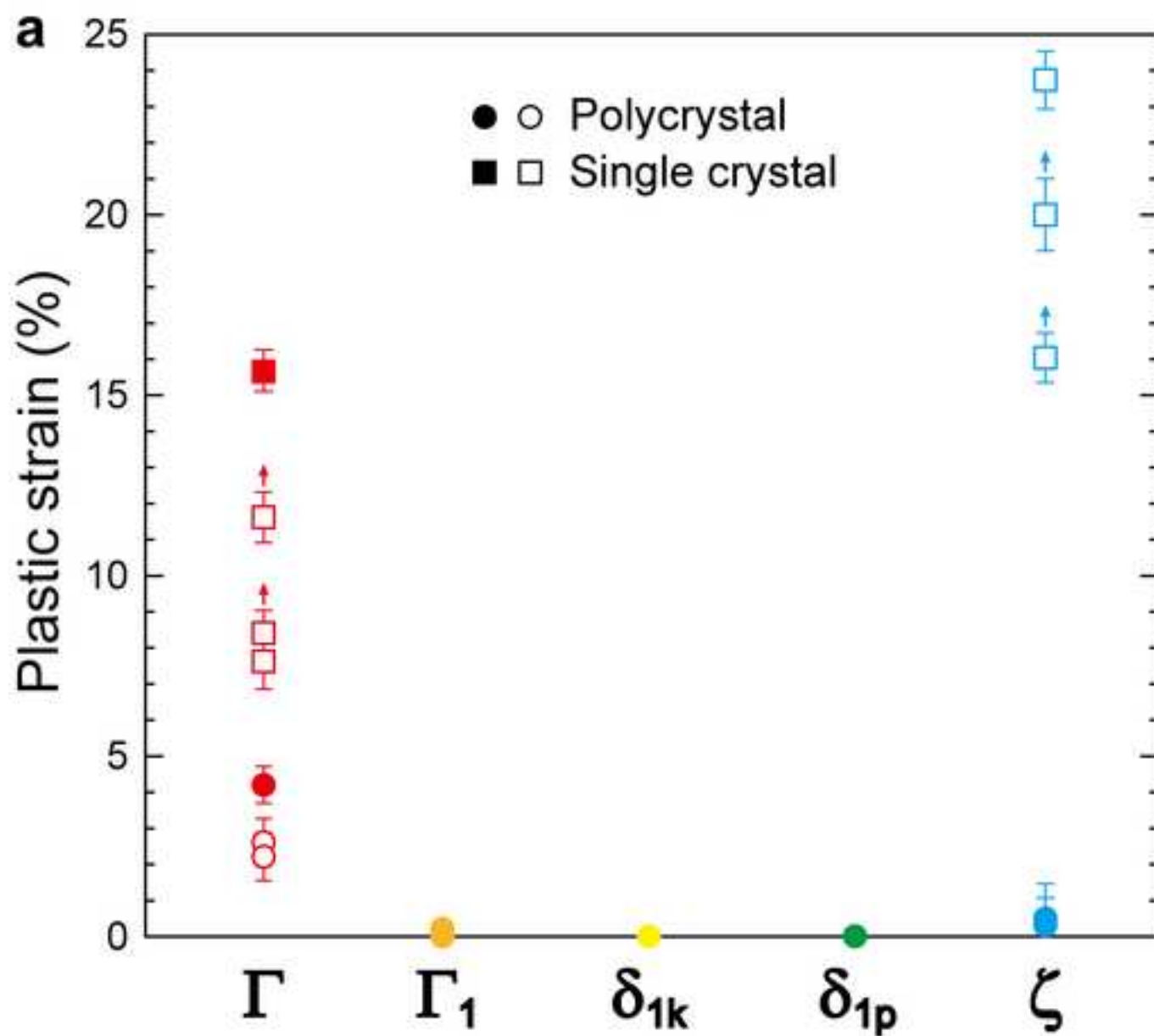
Γ and ζ phases tend to retard the crack propagation and hold ruptured fragments of the Γ_1 and δ_{1k}/δ_{1p} phases by their plastic deformation. In a high strain regime, intergranular cracks are introduced into the ζ phase as the phase does not satisfy the von Mises criterion [23, 24].

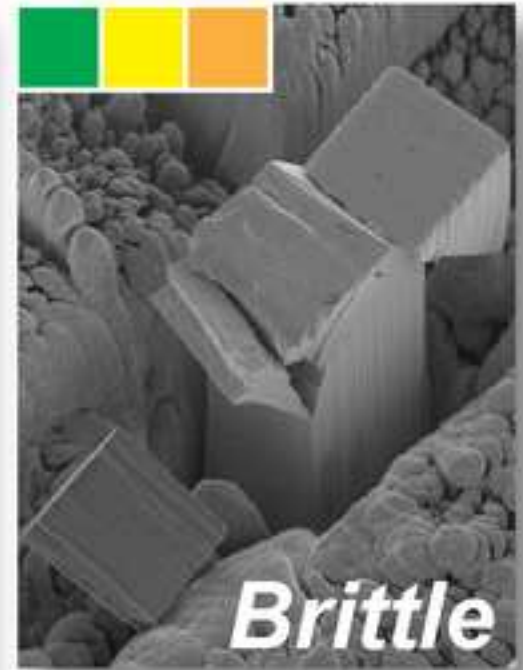
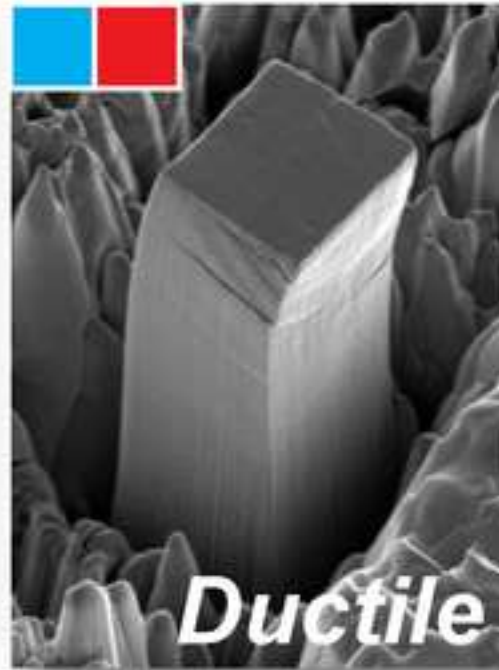
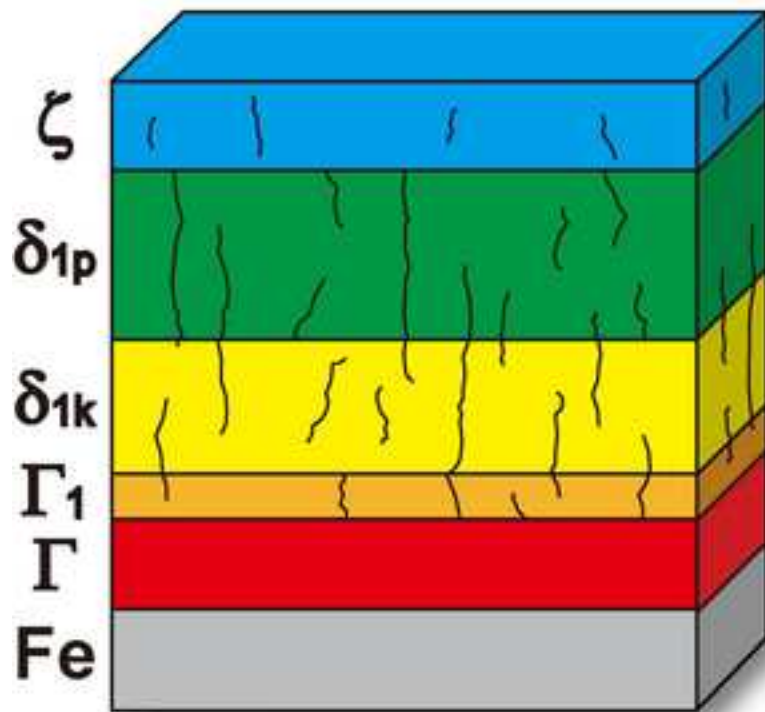


Figure(s)
[Click here to download high resolution image](#)



Figure(s)
[Click here to download high resolution image](#)





Supplementary Material

[Click here to download Supplementary Material: Supplementary_Information.pdf](#)

